2020 28th Mediterranean Conference on Control and Automation (MED)
15-18 September, 2020 - Saint-Raphaël, France

On Determining Shortest Path in Joint Space of a Cable-Driven Parallel Robot for Point-to-Point Motion

Utkarsh A. Mishra, Ishan Chawla and Pushparaj Mani Pathak

Abstract— **This paper presents a methodology to determine the shortest path in the joint space of a cable-driven parallel robot for point-to-point motions. The formulation is based on the joint space domain i.e., cable length and the shortest path in joint space is determined between the two points. The path is constrained by the 4th degree polynomial in the Cartesian space and the objective function representing the total path length in the joint space is formulated. The parameters of the path are obtained by minimizing the objective function using genetic algorithm while satisfying the non-negative cable tension constraints. The proposed methodology is validated using a 3-DOF planar and a 6-DOF spatial cable-driven robot. The obtained optimized shortest path is compared to a straight-line path and the results obtained shows a significant reduction in the joint space path length of a cable-driven parallel robot for the optimized path. The reduction will be even more significant for the large-scale cable-driven parallel robot.**

I. Introduction

Cable-driven parallel robots (CDPR) belong to the category of parallel kinematic structures, linked with lightweight flexible cables. They comprise of a moving platform, the end effector, and a base frame. These components are connected by multiple cables in parallel and are operated by the means of actuators which can retract and release cables. Compared to serial manipulators, the motions of the end effector are controlled by cables instead of rigid links. Such types of robots can be well equipped with attachments like hooks, cameras, grippers, etc. All these flexibilities have enabled CDPRs to be well suited for various applications with small to very large workspaces. Also, they possess some desirable characteristics, high-speed motion [1], high payload to weight ratio as well as significantly large workspaces. Such a simple design makes them mobile and economical. With respect to their applications, several authors have introduced interesting works in the last years. Significant examples include NIST RoboCrane [2] and SkyCam [3]. Also, remarkable works are presented as support structures for large telescopes [4] and rescue operations [5]. CDPRs have also been used in rehabilitation robotics [6].

As mentioned before, the cables are retracted or released by means of actuators or winches. Cable motions play a significant role in directly affecting the kinematics and dynamics of the CDPR system. Hence, path planning is a major concern. Various researchers have been proposing optimal trajectories based on multiple governing parameters. For a less complex case, we will consider massless cables, such that they always remain straight between the anchor points on the end-effector and the fixed frame. Generally, in kinematic modelling of CDPRs, such a straight-line model for describing the cable profile is sufficient for most redundantly constrained robots [7]. Moreover, there are a lot of constraints on cable tensions as cables can only exert positive tensions. All such conditions result in a constrained motion.

Total time, net energy consumption along with bounded tension on cables are some major governing parameters for path optimization as chosen by several researchers. Cable tensions, having natural constraints of being always positive, are used in various ways along with some added maximum and minimum values. Gosselin *et al.* [8] contributed to the dynamic planning of a 2-DOF cable-suspended parallel robot (CSPR). An approach of defining parametric feasible Cartesian trajectories was introduced and bounded tension constraints were considered to extend use of CDPR to areas outside workspaces. Also, Gosselin and Foucault [9] presented a similar extended point-to-point (P2P) motion for 2-DOF planar CSPR applicable beyond their static workspaces. The trajectory was modelled based on polynomial and trigonometric functions for intermediate points, where the former one has to be discretized for verification whereas the later one can be verified by algebraic expressions. Discussing about path planning, the traversal time is a major concern for industrial tasks. Recently, Barbazza *et al.* [10] came up with an optimized trajectory planning algorithm for a pick and place operation. The work focussed on replacing the horizontal movement between pick and place positions by an optimized transfer movement based on traversal time. Previously, Trevisani [11] considered bounded positive cable tensions to plan the time optimal trajectory for an under-constrained planar cable-robot by developing correlations from tensions to velocities and accelerations of the end effector. Thus, it is justified that researchers have presented interesting works exploiting the time and tension constraints. Along with these two, energy consumption plays a vital role in path planning too. Bamdad [12] worked on finding the time-energy optimal trajectory. He developed an analogy from works on serial manipulators and implemented the Pontryagin Maximum Principle. Barnett and Gosselin [13] defined two significant methods based on time-optimal trajectory planning (TOTP) and a modified minimum-time trajectory shaping (MTTS). An optimal trajectory was developed using the fusion of the above two methods. Tempel *et al.* [14] presented a programming concept for CDPR at EXPO 2015. The complete process workspace analysis to the obtaining of energy optimal trajectory was presented. The main goal is the maximum possible exploitation of workspace to achieve desired motions smoothly. Also, discussing of energy based optimizations, Zhang *et al.* [15] used quintic polynomials on desired intermediate points to get dynamic

*Resrach supported by SPARC, MHRD, India
Utkarsh A. Mishra, Ishan Chawla and Pushparaj Mani Pathak are with the Indian Institute of Technology, Roorkee-247667, Uttarakhand, India (phone: +917837030449; e-mail: umishra@me.iitr.ac.in, ichawla@me.iitr.ac.in and pushparaj.pathak@me.iitr.ac.in).

planning for 3-DOF spatial CSPR in order to maintain safety of cable tensions and reduce travel time. This recent study shows that, there are active works going on in this path optimization domain and there are still many unexplored areas that can act as useful optimization measures.

In this paper, the methodology to determine the shortest path in joint space for a cable-driven parallel robot is proposed. The cost function for minimizing the path length is formulated and the necessary constraints for the problem are defined. The wrench-feasibility constraints have also been added to the optimization problem in order to ensure the reliable operation of the robot. The optimization is performed using genetic algorithm using the proposed objective function and constraints. The proposed methodology is validated for a planar redundant 3 DOF cable-driven parallel robot.

The "shortest path" in joint space is interpreted to be the fastest path and/or energy efficient path. However, this interpretation is incomplete, as the path does not have any time or energy information. The "shortest path" can be the "fastest path" if the end-effector is moving "quasi-statically" or if the actuators only move at a "constant" positive and negative velocity, where the total time is directly dependent on the total displacement of the joint angles. The quasi-static assumption is viable for application like 3D printing where the speed of the end-effector will be "slow" enough to be considered static. Therefore, the proposed path can be inferred as the fastest path in such scenario and can be applied for "idle motions" of the end-effector during 3D printing.

The paper is organized as follows: Section II formulates the problem statement and a generalized objective function was constructed for optimization. Section III discusses the simulation results of 3-DOF planar CDPR. The section describes the effectiveness of the optimal planning methodology considered by the authors, through numerical investigations. The paper finally concludes in Section IV.

II. PROPOSED METHODOLOGY

A. Wrench-Feasibility Constraint

Consider a cable-driven parallel robot consisting of an end-effector/mobile-platform manipulated by means of n_c number of cables. Let, the position vector $\mathbf{a}_i$ and the position vector $\mathbf{b}_i$ represents the position of i^{th} cable anchor point with respect to global coordinate frame $\{O\}$ and local coordinate frame $\{E\}$, respectively. The local coordinate frame $\{E\}$ is attached to the center of mass of the end-effector. Vector $\mathbf{r}$ and transformation matrix $\mathbf{R}$ represents the position and orientation of the end-effector with respect to the global frame $\{O\}$. Let, A_i represents the support point of i^{th} cable. The schematic diagram of the CDPR kinematics is shown in Figure 1. The i^{th} cable length vector $\mathbf{l}_i$ pointing away from the end-effector can be obtained using closed-loop kinematic constraints as [16]:

$$\mathbf{l}_i = \mathbf{a}_i - \mathbf{r} - \mathbf{R}\,\mathbf{b}_i \tag{1}$$

The unit vector $\mathbf{u}_i$ in the direction of length vector $\mathbf{l}_i$ can be obtained by:

$$\mathbf{u}_i = \frac{\mathbf{l}_i}{\|\mathbf{l}_i\|_2} \tag{2}$$

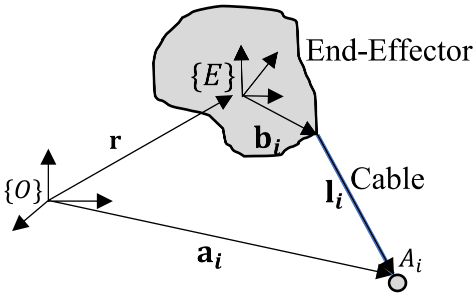

Figure 1: Schematic diagram for the kinematics of CDPR

Let, $\mathbf{f}$ represents a wrench vector which is composed of force vector $\mathbf{f_p}$ and torque vector $\boldsymbol{\tau}_p$ applied at the center of mass of the end-effector, respectively. In order to statically balance the end-effector, the following equation must be satisfied:

$$\underbrace{\begin{bmatrix} \mathbf{u_1} & \cdots & \mathbf{u}_{n_c} \\ \mathbf{b_1} \times \mathbf{u_1} & \cdots & \mathbf{b}_{n_c} \times \mathbf{u}_{n_c} \end{bmatrix}}_{\mathbf{W(r,R)}} \underbrace{\begin{bmatrix} t_1 \\ \vdots \\ t_{n_c} \end{bmatrix}}_{\mathbf{t}} + \underbrace{\begin{bmatrix} \mathbf{f_p} \\ \boldsymbol{\tau}_p \end{bmatrix}}_{\mathbf{f}} = \mathbf{0} \tag{3}$$

where $\boldsymbol{W}$ represents the wrench matrix which transforms cable tensions form joint space into the end-effector wrench in the Cartesian space and vector $\boldsymbol{t} = [t_1, \dots, t_{n_c}]^T$ denotes the cable tension vector. In compact matrix-vector form, (3) can be abbreviated as:

$$\mathbf{W(r,R)t + f = 0} \tag{4}$$

Since, cables can only push and not pull, the tension in the cable should be always non-negative in order to control the end-effector. Apart from that, the cable tension must lie within a range bounded by minimum tension bound $\mathbf{t}_{min}$ and maximum tension bound $\mathbf{t}_{max}$. The minimum tension bound $\mathbf{t}_{min}$ is desirable to ensure reliable, tangle-free operation of the robot while the maximum tension bound $\mathbf{t}_{max}$ is used to consider maximum torque limitation of the actuator. This is where the term wrench-feasibility comes into play. For an end-effector pose to be wrench-feasible, the following condition must be satisfied [17], [18]:

$$\mathbf{W(r,R)t + f = 0} \;\; \ni \mathbf{0} < \mathbf{t}_{min} \le \mathbf{t} \le \mathbf{t}_{max}\,, \tag{5}$$

Equation (5) states that a pose is said to be wrench-feasible for wrench $\mathbf{f}$, if for that pose, cables can statically balance the end-effector such that the cable tension in all the cables are within the non-negative range bounded by $\mathbf{t}_{min}$ and $\mathbf{t}_{max}$.

Thus, the wrench-feasibility condition given by (5) must be satisfied for all the poses in the designed path. To check for wrench-feasibility of redundant CDPR, multiple algorithms have been proposed in the literature. Some of the methods. Linear programming [19], closed-form algorithm [20] and puncture method [21] are some of the algorithms for checking wrench-feasibility. In this work, linear programming has been used to check the wrench-feasibility of a given pose. The linear programming problem can be defined as:

$$\min \mathbf{c^T t} \;\; \text{such that}\; \mathbf{Wt} = -\mathbf{f} \;\text{and}\; \mathbf{t}_{min} \le \mathbf{t} \le \mathbf{t}_{max} \tag{6}$$

where $\mathbf{c}$ can be chosen to be any arbitrary vector as the objective is to just find any solution satisfying the constraints. Thus, the presented wrench-feasibility condition will act as a constraint to the optimization problem discussed in the next subsection.

B. Formulating the Optimization Problem

The primary objective of this section is to determine the shortest path in the joint space of the robot between the user specified initial pose $\mathbf{X_{initial}}$ and final point $\mathbf{X_{final}}$ such that the wrench-feasibility constraint discussed in the previous subsection is satisfied for all the poses in the path. For a 6 DOF robot, the pose vector $\mathbf{X}$ refers to the vector $[x, y, z, \alpha, \beta, \gamma]^{\boldsymbol{T}}$, where x, y and z represents the position and α, β and γ denotes the Euler angles of the local coordinate system $\{E\}$ attached the end-effector with respect to the world coordinate system $\{O\}$. The position vector $\mathbf{r}$ and the rotation matrix $\mathbf{R} \in \mathrm{SO}(3)$ are related to the pose vector $\mathbf{X}$ as:

$$\mathbf{r} = [x, y, z]^T \tag{7}$$

$$\mathbf{R} = \begin{bmatrix} \cos\alpha\cos\beta & \cos\alpha\sin\beta\sin\gamma - \sin\alpha\cos\gamma & \cos\alpha\sin\beta\cos\gamma + \sin\alpha\sin\gamma \\ \sin\alpha\cos\beta & \sin\alpha\sin\beta\sin\gamma + \cos\alpha\cos\gamma & \sin\alpha\sin\beta\cos\gamma - \cos\alpha\sin\gamma \\ -\sin\beta & \cos\beta\sin\gamma & \cos\beta\cos\gamma \end{bmatrix} \tag{8}$$

In order to determine the shortest path in joint space, the path $\mathbf{X}(u)$ is first parametrized as a 4^{th} degree polynomial with a parameter u, such that $\mathbf{X}(0) = \mathbf{X_{initial}}$ and $\mathbf{X}(1) = \mathbf{X_{final}}$ where $u \in [0, 1]$. Polynomial of higher degree can also be chosen however, that would increase the number of parameters to be optimized and hence the computational time of optimization will be increased. On the other hand, lower degree polynomial would reduce the flexibility of the optimization to determine shortest path.

The parameterization of the orientation is mostly done using Euler angles in the robotics literature [22]. However, the Euler angles undergo problems such as gimbal lock [23]. The spherical unit quaternion parameterization has been used by many researchers to avoid problems in Euler angle parameterization. Additionally, the unit quaternions parameterization has been observed to give smooth transformation in orientation [24]. However, the range of orientation of end-effector is generally low in the CDPRs due to collision of cable with the end-effector or with other cables. In that case, Euler angles parameterization can also be used effectively without encountering the problem of gimbal lock [23]. Thus, Euler angle parameterization is employed in this paper.

The parametrized path in terms of a 4^{th} degree polynomial can be written in matrix form:

$$\begin{bmatrix} x(u) \\ y(u) \\ z(u) \\ \alpha(u) \\ \beta(u) \\ \gamma(u) \end{bmatrix} = \begin{bmatrix} p_{x0} & p_{x1} & p_{x2} & p_{x3} & p_{x4} \\ p_{y0} & p_{y1} & p_{y2} & p_{y3} & p_{y4} \\ p_{z0} & p_{z1} & p_{z2} & p_{z3} & p_{z4} \\ p_{\alpha0} & p_{\alpha1} & p_{\alpha2} & p_{\alpha3} & p_{\alpha4} \\ p_{\beta0} & p_{\beta1} & p_{\beta2} & p_{\beta3} & p_{\beta4} \\ p_{\gamma0} & p_{\gamma1} & p_{\gamma2} & p_{\gamma3} & p_{\gamma4} \end{bmatrix} \begin{bmatrix} 1 \\ u \\ u^2 \\ u^3 \\ u^4 \end{bmatrix} \tag{9}$$

where the coefficients $p_{\eta i}$ represents the coefficients of the path such that $\eta \in \mathbf{X}$ and $i = 0$ to 4. In compact matrix notation, (9) can be re-written as:

$$\mathbf{X}(u) = \mathbf{P}\,\mathbf{U}(u) \tag{10}$$

In order to satisfy the initial condition ($\mathbf{X}(0) = \mathbf{X_{initial}}$) and final condition ($\mathbf{X}(1) = \mathbf{X_{final}}$), some constraints can be imposed on the coefficients, such as:

$$p_{\eta0} = \eta_{initial} \tag{11}$$

where (11) corresponds to the case of u = 0 and (12) is formulated in a similar way for u = 1.

$$\sum_{i=1}^{4} p_{\eta i} = \eta_{final} - \eta_{initial}\ , \ \eta \in \mathbf{X} \tag{12}$$

Thus, the objective of the optimization is to optimize the coefficients $p_{\eta i}$ in order to minimize a cost function while satisfying the constraints given by (6), (11) and (12). The cost function is chosen to minimize the path length in the joint space of CDPR.

C. Formulating the Cost Function of Optimization

The path length in the joint space corresponds the path taken by cable lengths during the path. This is done by determining the total variation in the length of the cables while following the path. The length of the cable can be obtained by taking 2-norms on both sides of (1) as:

$$|\,\boldsymbol{l}_i\,|^2 = |\,\boldsymbol{a}_i - \boldsymbol{r} - \boldsymbol{R}\,\boldsymbol{b}_i\,|^2 \tag{13}$$

Now, differentiating (13) with respect to parameter u yields:

$$2\,|\,\mathbf{l_i}\,|\,\frac{d(\mathbf{l_i})}{du} = 2\,|\,\boldsymbol{a}_i - \boldsymbol{r} - \boldsymbol{R}\,\boldsymbol{b}_i\,|\,\frac{\boldsymbol{d}(|\,\boldsymbol{a}_i - \boldsymbol{r} - \boldsymbol{R}\,\boldsymbol{b}_i\,|)}{du} \tag{14}$$

Equation (14) can be re-written in terms of state vector $\mathbf{X}$ as:

$$\frac{d(\mathbf{l_i})}{du} = \frac{|\,\boldsymbol{a}_i - \boldsymbol{r} - \boldsymbol{R}\,\boldsymbol{b}_i\,|}{|\,\mathbf{l_i}\,|}\,\frac{d(|\,\boldsymbol{a}_i - \boldsymbol{r} - \boldsymbol{R}\,\boldsymbol{b}_i\,|)}{d\,\mathbf{X}}\,\frac{d\,\mathbf{X}}{du} \tag{15}$$

The path length of one cable can be determined by the length of the curve taken by the length of the cable from initial to final pose. After formulating the change in the length of i^{th} cable for a small translation and rotation of the end-effector, $d(\mathbf{l_i})$ was calculated for the joint space of the cable. Hence, the overall path length of the i^{th} cable (in joint space) for the total path in Cartesian space was calculated as:

$$\Delta\mathbf{l_i} = \int_0^1 \sqrt{1 + \left(\frac{d(\mathbf{l_i})}{d(u)}\right)^2}\, du \tag{16}$$

where $\Delta\mathbf{l_i}$ corresponds to the path length of the i^{th} cable in joint space. Finally, after substituting $\frac{d(\mathbf{l_i})}{du}$ in (16) from (15) gives the exact formulation of the path length.

$$\Delta\mathbf{l_i} = \int_0^1 \sqrt{\mathbf{1} + \left(\frac{|\,\boldsymbol{a}_i - \boldsymbol{r} - \boldsymbol{R}\,\boldsymbol{b}_i\,|}{|\,\mathbf{l_i}\,|}\frac{d(|\,\boldsymbol{a}_i - \boldsymbol{r} - \boldsymbol{R}\,\boldsymbol{b}_i\,|)}{d\,\mathbf{X}}\frac{d\,\mathbf{X}}{d(u)}\right)^2}\, du \tag{17}$$

Minimizing the above integral for each of the cables will eventually lead to the shortest path of that particular cable in joint space. Thus, the final objective function to minimize the total path length of each cable in joint space is given in (18).

$$\boldsymbol{Z} = minimum \sum_{i=1}^{n} \Delta\mathrm{l_i} \tag{18}$$

Therefore, the optimized shortest path can be obtained my minimizing the cost function (given by (18)) while satisfying the wrench-feasibility constraints (given by (6)). Genetic Algorithm (GA) optimization is used in this paper. GAs have a clear advantage with large solution spaces due to their robustness in converging.

III. RESULTS AND DISCUSSIONS

In this section, the proposed methodology is validated on a planar 3-DOF and a spatial 6-DOF cable-driven parallel robot for determining the shortest path in joint space, a schematic diagram of which is shown in figure 5.

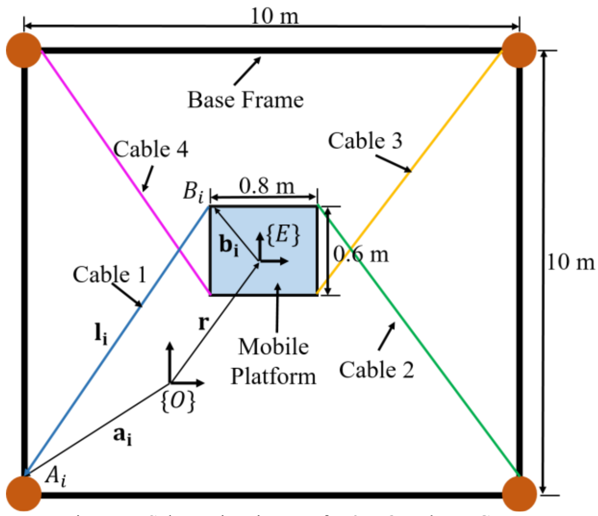

Figure 5: Schematic Diagram for 3-DOF Planar CDPR

A. 3-DOF Planar CDPR

The geometry of the cable-driven parallel robot is defined by a rectangular end-effector of dimensions 0.6 m x 0.8 m and a fixed square frame of side 10 m. The mass of the end-effector is considered to be $m = 50\ Kg$. The anchor points at the frame and end-effector are taken at the corner of the frame and in crossed-configuration. The pose of the end-effector is represented by the pose vector $\mathbf{X} = [\,x, z, \beta]^T$ is considered, where, β represents the orientation of the end-effector. The orientation β of the end-effector is constrained to be within $\left(-\frac{\pi}{4}, \frac{\pi}{4}\right)$ in order to prevent collision of cables with the end-effector. It is desired to determine the shortest path in joint space between the initial pose $\boldsymbol{X_{initial}} = [\,3, 8, 0\,]^T$ and final pose $\boldsymbol{X_{final}} = [\,8, 2, 0\,]^T$.

TABLE I. PARAMETERS FOR GA

Parameters	***Values***
Population Size	200
Selection Policy	Roulette Wheel
Crossover Rate	80%
Mutation Rate	1%
Number of Generations	200

The objective of the optimization is to minimize the cost function given in (18) while satisfying the wrench-feasibility given by (6) and initial-final pose constraints given by (11) and (12). The wrench vector $\mathbf{f} = [0, -mg, 0]^T$ with minimum tension bound $t_{min} = 100$ N and maximum tension bound $t_{max} = 1500$ N is considered for wrench-feasibility constraints where $g = 9.8\ \mathrm{m/s^2}$ denotes the acceleration due to gravity. The genetic algorithm is used for optimization with random initial population. The parameters of the genetic algorithm are given in Table I.

Using optimization, the optimized coefficients $p_{\eta i}$ are obtained which are further incorporated in (11) to give the final path $\mathbf{X}(u)$ where $u \in [0, 1]$. Figure 6 shows the optimized path of the end-effector. The end-effector is shown at various poses throughout the path given by red line.

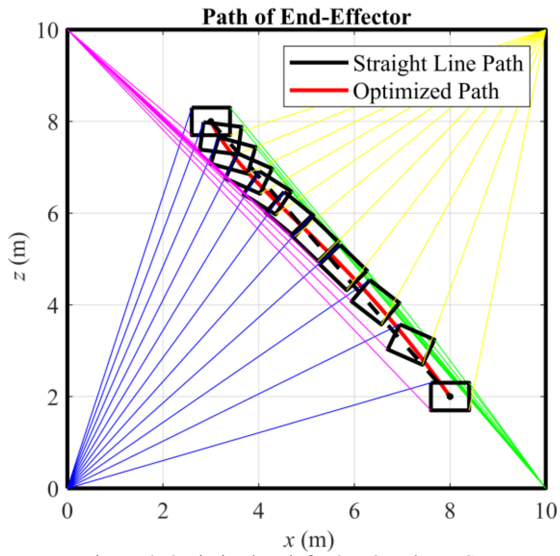

Figure 6: Optimized Path for 3-DOF Planar CDPR

An optimized path consisting of a curved path with a continuous change of orientation was observed. The variation of orientation (β) of end-effector is shown in Figure 7. From Figure 7, it has been observed that the orientation of the end-effector is fully exploited in order to get a shortest path in joint space. Furthermore, the optimized path is compared to the straight-line path in Cartesian space, to analyze the effect of the path length in joint space.

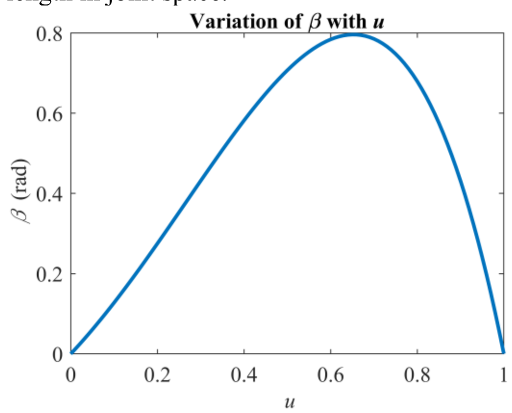

Figure 7: Variation of orientation angle (β) of end-effector with u for 3-DOF CDPR setup

Figure 8 shows the comparison of joint space path for optimized and straight-line path. From the results it can be observed that the optimized path taken by cable 1 and cable 3 is shorter than the straight-line path. However, for cable 2 and cable 4, the paths appears to be same in length. Overall, the optimized path is observed to be shorter than the straight-line path. The visual observations are validated by the calculated path lengths for each cable, shown in Table II, where a shorter path length is observed for cable 1 and cable 3 using an optimized path when compared to straight-line path. Overall, the total reduction of 1.78 m is obtained using an optimized path compared to the straight-line path.

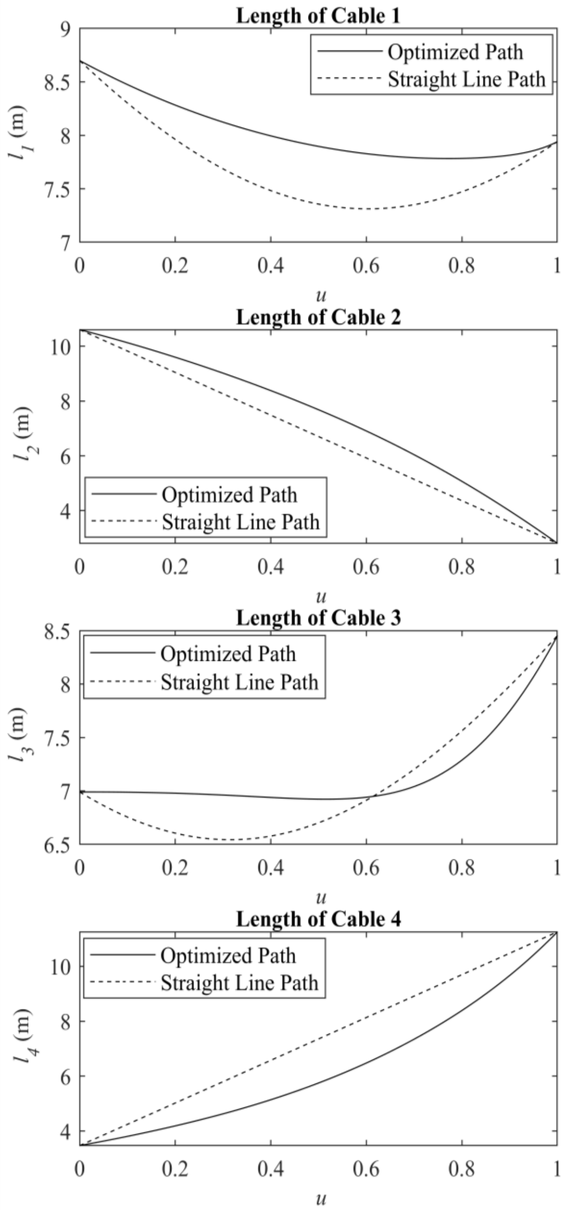

Figure 8: Lengths of all the cables from the given initial to final state, in joint space, with respect to u

TABLE II. PATH LENGTHS IN JOINT SPACE

Path	Δl_1	Δl_2	Δl_3	Δl_4	$\sum_{i=1}^{4} \Delta l_i$
Optimized	1.01	7.80	1.59	7.78	18.18
Straight Line	2.02	7.80	2.36	7.78	19.96

All lengths in meters (m)

B. *6-DOF Spatial CDPR*

The geometry parameters of a 6-DOF spatial CDPR consists of an end-effector of dimension 0.8 m × 0.6 m × 0.6 m and a fixed frame of dimension 10 m × 10 m × 10 m. The mass of the end-effector is $m = 50\,kg$ and the cable configuration is maintained to be crossed along the z-axis. Now, the pose of the end-effector is represented by the pose vector $\mathbf{X} = [\,x, y, z, \alpha, \beta, \gamma]^T$, where, α, β and γ represent the Euler angle orientation of the end-effector. Unlike the planar case, a cable end-effector collision avoidance criterion is considered in this case to bound orientation to end-effector. It is desired to determine the shortest path in joint space between the initial pose $\boldsymbol{X_{initial}} = [\,2, 1, 1.5, 0, 0, 0]^{\boldsymbol{T}}$ and final pose $\boldsymbol{X_{final}} = [\,8, 6, 7, 0, 0, 0]^{\boldsymbol{T}}$.

The objective function was minimized in a similar manner with the help of the initial conditions and the wrench feasibility constraints. A minimum tension bound $t_{min} = 100\,N$ and maximum tension bound $t_{max} = 1500\,N$ is considered with a wrench vector $\mathbf{f} = [0,0,-mg,0,0,0]^T$ for the wrench feasibility constraints. As the number of optimizable variables, $p_{\eta i}$ increased from 12 (for planar) to 24 (for spatial), population size of 500 is considered for the genetic algorithm based optimization while keeping all other parameters according to Table I. The optimized coefficients were used to get the final path traversed by the end-effector. This path is shown in Figure 9 with local frame orientation markers for various poses of the end-effector.

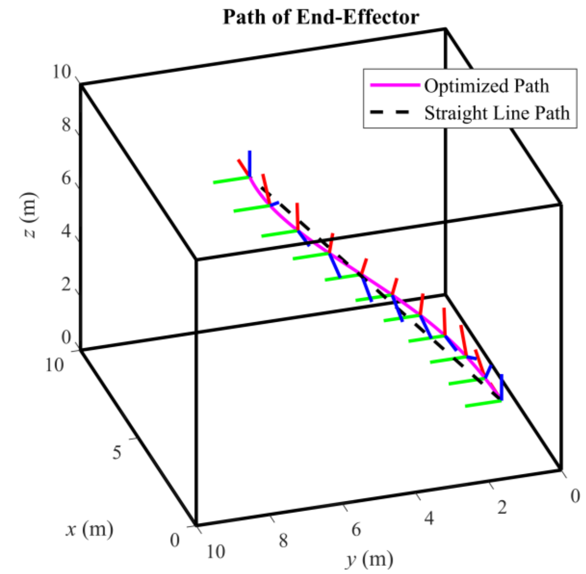

Figure 9: Optimized Path for 6-DOF Spatial CDPR

Again, a continuous path with change in orientation was observed. Only the variation in Euler angle β is observed whereas the other two Euler angles remain zero for the complete optimized path. The variation in β is shown in Figure 10. This is because of the un-crossed symmetry about the plane perpendicular to x and y-axis (red and green axis in local frame respectively) passing through the centre of the end-effector. In addition to this, a greater length along the x-axis i.e. 0.8 m as compared to 0.6 m along y-axis resulted in a greater change of length for rotation about y-axis. Thus, with a greater variation in β, more reduction was achieved and hence the other two angles remain zero for the entire path.

A similar length analysis as that of the planar case was done for the spatial case as well. However, due to space limitations the plots have not been included in the paper. The straight line path corresponds to a total change in path (i.e., $\sum_{i=1}^{8} \Delta l_i$) of 40.83 m whereas the optimized path reduced the total change in path length to 38.82 m. Hence, a total reduction of 2.01 m is achieved as compared to the straight-line path in Cartesian space.

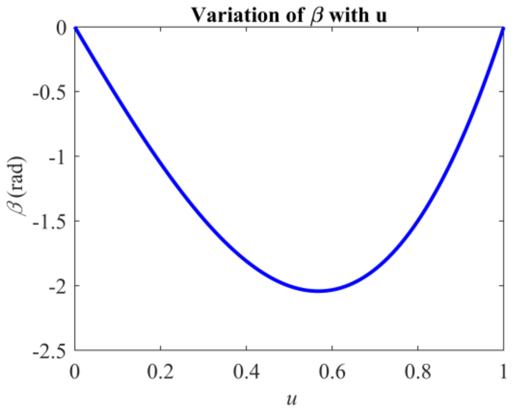

Figure 10: Variation of orientation angle (β) of end-effector with u for 6-DOF Spatial CDPR setup

Thus, a significant reduction in joint space path length is observed for both planar and spatial cases, using the proposed approach. This would be very useful for repetitive operations or large-scale robots.

IV. CONCLUSION

This paper presented a methodology to determine the shortest path between the two points in the joint space of a cable-driven parallel robot. The 4th degree polynomial parametrization of the path has been done in the Cartesian space and the objective function representing the total path length in the joint space has been formulated. The wrench-feasibility constraints have been added to the optimization to keep the tension in the cables in the non-negative bounded range during the path. The proposed methodology has been validated on a 3-DOF planar as well as on a 6-DOF spatial cable-driven robot and the obtained optimized shortest path has been compared to a straight-line path. The obtained results show a reduction of 1.78 m in the joint space path length of a 3-DOF planar cable-driven robot and 2.01 m for the 6-DOF spatial robot. The orientation of the end-effector was found to play a significant role in reducing the path length in joint space. Since cable-driven parallel robots are known for their large workspaces, a large reduction can be obtained for the large-scale cable-driven parallel robot. In future, the authors plan to validate the proposed methodology on the experimental setup.

ACKNOWLEDGMENT

This research was undertaken through the scheme for promotion of academic and research collaboration (SPARC) project funded by MHRD, Government of India, under Project No. SPARC/2018-2019/P713/SL. IIT Roorkee, India, IIT Kharagpur, India and Queen's University, Canada, are the collaborating institutions in the above-mentioned project.

REFERENCES

[1] S. Kawamura, W. Choe, S. Tanaka, and S. R. Pandian, "Development of an ultrahigh speed robot FALCON using wire drive system," in *International Conference on Robotics and Automation*, 1995, pp. 215–220.

[2] J. Albus, R. Bostelman, and N. Dagalakis, "The NIST robocrane," *J. Robot. Syst.*, vol. 10, no. 5, pp. 709–724, 1993.

[3] L. L. Cone, "Skycam: an Aerial Robotic Camera System.," *Byte*, vol. 10, no. 10, 1985.

[4] R. Nan, "Five hundred meter aperture spherical radio telescope (FAST)," *Sci. China, Ser. G Phys. Astron.*, vol. 49, no. 2, pp. 129–148, 2006.

[5] J. P. Merlet and D. Daney, "A portable, modular parallel wire crane for rescue operations," in *International Conference on Robotics and Automation*, 2010, pp. 2834–2839.

[6] G. Rosati, M. Andreolli, A. Biondi, and P. Gallina, "Performance of cable suspended robots for upper limb rehabilitation," in *International Conference on Rehabilitation Robotics*, 2007, pp. 385–392.

[7] X. Tang, "An overview of the development for cable-driven parallel manipulator," *Adv. Mech. Eng.*, 2014.

[8] C. Gosselin, P. Ren, and S. Foucault, "Dynamic trajectory planning of a two-DOF cable-suspended parallel robot," in *International Conference on Robotics and Automation*, 2012, pp. 1476–1481.

[9] C. Gosselin and S. Foucault, "Dynamic point-to-point trajectory planning of a two-DOF cable-suspended parallel robot," *IEEE Trans. Robot.*, vol. 30, no. 3, pp. 728–736, 2014.

[10] L. Barbazza, F. Oscari, S. Minto, and G. Rosati, "Trajectory planning of a suspended cable driven parallel robot with reconfigurable end effector," *Robot. Comput. Integr. Manuf.*, vol. 48, no. 1, pp. 1–11, 2017.

[11] A. Trevisani, "Underconstrained planar cable-direct-driven robots: A trajectory planning method ensuring positive and bounded cable tensions," *Mechatronics*, vol. 20, no. 1, pp. 113–127, 2010.

[12] M. Bamdad, "Time-energy optimal trajectory planning of cable-suspended manipulators," in *Mechanisms and Machine Science*, 2013, pp. 41–51.

[13] E. Barnett and C. Gosselin, "Time-optimal trajectory planning of cable-driven parallel mechanisms for fully specified paths with G1-discontinuities," *J. Dyn. Syst. Meas. Control*, vol. 137, no. 7, pp. 1–12, 2015.

[14] P. Tempel, F. Schnelle, A. Pott, and P. Eberhard, "Design and programming for cable-driven parallel robots in the German Pavilion at the EXPO 2015," *Machines*, vol. 3, no. 3, pp. 223–241, 2015.

[15] N. Zhang, W. Shang, and S. Cong, "Dynamic trajectory planning for a spatial 3-DoF cable-suspended parallel robot," *Mech. Mach. Theory*, vol. 122, pp. 177–196, 2018.

[16] A. Pott, *Cable-driven parallel robots: Theory and application*. 2018.

[17] M. Gouttefarde, J. P. Merlet, and D. Daney, "Wrench-feasible workspace of parallel cable-driven mechanisms," in *International Conference on Robotics and Automation*, 2007, pp. 1492–1497.

[18] I. Chawla and P. M. Pathak, "Performance enhancement of interval-analysis-based-methods for wrench-feasible workspace computation of cable-driven parallel robot," in *ACM International Conference Proceeding Series*, 2019.

[19] C. Gosselin and M. Grenier, "On the determination of the force distribution in overconstrained cable-driven parallel mechanisms," *Meccanica*, vol. 46, no. 1, pp. 3–15, 2011.

[20] L. Notash, "Designing positive tension for wire-actuated parallel manipulators," in *Mechanisms and Machine Science*, 2013.

[21] K. Müller, C. Reichert, and T. Bruckmann, "Analysis of a real-time capable cable force computation method," in *Mechanisms and Machine Science*, 2015.

[22] J. J. Craig, *Introduction to Robotics: Mechanics and Control*. Addison Wesley Longman, 1995.

[23] J. J. Kuffner, "Effective sampling and distance metrics for 3D rigid body path planning," in *International Conference on Robotics and Automation*, 2004, pp. 1–6.

[24] D. Q. Huynh, "Metrics for 3D rotations: Comparison and analysis," *J. Math. Imaging Vis.*, vol. 35, no. 2, pp. 155–164, 2009.